



RESEARCH ARTICLE

Functional correlates of motor control impairments in multiple sclerosis: A 7 Tesla task functional MRI study

Myrte Strik^{1,2}  | Camille J. Shanahan¹ | Anneke van der Walt³ |
 Frederique M. C. Boonstra³ | Rebecca Glarin¹ | Mary P. Galea¹ |
 Trevor J. Kilpatrick^{4,5,6} | Jeroen J. G. Geurts² | Jon O. Cleary⁷ |
 Menno M. Schoonheim²  | Scott C. Kolbe^{1,3}

¹Department of Medicine and Radiology, University of Melbourne, Parkville, Australia

²Department of Anatomy and Neurosciences, MS Center Amsterdam, Amsterdam Neuroscience, Amsterdam UMC, Vrije Universiteit Amsterdam, Amsterdam, the Netherlands

³Department of Neurosciences, Central Clinical School, Monash University, Melbourne, Australia

⁴Florey Institute of Neuroscience and Mental Health, Parkville, Australia

⁵Florey Department of Neuroscience and Mental Health, University of Melbourne, Parkville, Australia

⁶Department of Neurology, Royal Melbourne Hospital, Parkville, Australia

⁷Department of Radiology, Guy's and St. Thomas' NHS Foundation Trust, London, UK

Correspondence

Myrte Strik, Department of Medicine and Radiology, University of Melbourne, Parkville, Australia.

Email: mstrik@unimelb.edu.au

Funding information

Melbourne International Research Scholarship; Melbourne Neuroscience Institute Interdisciplinary Seed Grant

Abstract

Upper and lower limb impairments are common in people with multiple sclerosis (pwMS), yet difficult to clinically identify in early stages of disease progression. Tasks involving complex motor control can potentially reveal more subtle deficits in early stages, and can be performed during functional MRI (fMRI) acquisition, to investigate underlying neural mechanisms, providing markers for early motor progression. We investigated brain activation during visually guided force matching of hand or foot in 28 minimally disabled pwMS (Expanded Disability Status Scale (EDSS) < 4 and pyramidal and cerebellar Kurtzke Functional Systems Scores \leq 2) and 17 healthy controls (HC) using ultra-high field 7-Tesla fMRI, allowing us to visualise sensorimotor network activity in high detail. Task activations and performance (tracking lag and error) were compared between groups, and correlations were performed. PwMS showed delayed (+124 s, $p = .002$) and more erroneous (+0.15 N, $p = .001$) lower limb tracking, together with lower cerebellar, occipital and superior parietal cortical activation compared to HC. Lower activity within these regions correlated with worse EDSS ($p = .034$), lower force error ($p = .006$) and higher lesion load ($p < .05$). Despite no differences in upper limb task performance, pwMS displayed lower inferior occipital cortical activation. These results demonstrate that ultra-high field fMRI during complex hand and foot tracking can identify subtle impairments in lower limb movements and upper and lower limb brain activity, and differentiates upper and lower limb impairments in minimally disabled pwMS.

KEYWORDS

disability, lower limb, motor control, multiple sclerosis, task functional MRI, ultra-high field MRI, upper limb

This is an open access article under the terms of the Creative Commons Attribution-NonCommercial-NoDerivs License, which permits use and distribution in any medium, provided the original work is properly cited, the use is non-commercial and no modifications or adaptations are made.

© 2021 The Authors. *Human Brain Mapping* published by Wiley Periodicals LLC.

1 | INTRODUCTION

Multiple sclerosis (MS) is a progressive disease of the central nervous system characterised by neuroaxonal inflammation, demyelination and degeneration. Motor impairments are common and disabling, and include tremor, muscle weakness, loss of fine motor control, ataxia and loss of mobility (Coghe et al., 2019). Walking difficulties are a typical hallmark of MS and occur in most people with MS (pwMS) (80%) within 10–15 years (Souza et al., 2010), and upper limb impairments also eventually occur in up to 80% as well (Johansson et al., 2007), yet are less well clinically studied. Also, the degree of impairment of upper and lower limbs correlates only moderately (Coghe et al., 2019), suggesting at least partially divergent mechanisms of progression. Elucidating such mechanisms is important for formulating personalised treatment strategies, especially early in the disease when clinical signs of disability are minimal yet efficacious treatment has the best chance of avoiding significant neurological decline.

Lesion pathology and axonal loss in important sensorimotor pathways in the brain and spinal cord such as the corticospinal tracts (CST) (Hubbard, Wetter, Sutton, Pilutti, & Motl, 2016; Kerbrat et al., 2020) and corpus callosum (CC) (Iandolo et al., 2020; Kolasa et al., 2019; Ozturk et al., 2010) has been shown to correlate with disability as measured with clinical tests (Kerbrat et al., 2020; Kolasa et al., 2019), gait (Hubbard et al., 2016) and proprioception. However, complex motor control involves multi-modal sensory inputs including visual and proprioceptive (Iandolo et al., 2020) information that are integrated and recurrently connected to motor outputs and fine-tuned by sub-cortical structures such as the thalamus and cerebellum. Thus, it is likely that contributing factors to the progression of motor impairments in people with MS include both structural damage to key sensorimotor structures, as well as adaptive neurophysiological changes in broader sensory, motor and sub-cortical brain networks.

Functional MRI (fMRI) provides a useful means of studying changes in brain activity and putative neural compensations that contribute to the rate of progression of motor impairments. Task-based fMRI reveals regional brain activation indirectly via local changes in blood flow in the cortex driven by neural activity. Such studies have shown that changes in activation can predate changes in sensorimotor impairments and could provide early indicators of subsequent neurological decline (Filippi et al., 2004). Multiple studies in MS have reported altered patterns of brain activation with increased activation seen in regions typically devoted to simple (Filippi et al., 2004; Mezzapesa, Rocca, Rodegher, Comi, & Filippi, 2008; Rocca et al., 2003, 2005) and more complex motor tasks (Filippi et al., 2004; Rocca et al., 2005) as well as decreased activation in patients with greater disability (Ciccarelli et al., 2006) and over time (Pantano et al., 2005). The evolution of increased and decreased activation changes through the course of the disease is still unknown. However, key shortcomings of the extant literature lies in the type of task and the stronger focus on hand function (Mezzapesa et al., 2008; Rocca et al., 2003, 2005), which can easily be performed during scanning with simple tasks involving flexion and extension of the hand or fingers (Mezzapesa et al., 2008; Rocca et al., 2003, 2005). As such, there

is little known about the neural changes accompanying tasks involving complex motor control that provide better models of day-to-day motor functions.

Lower limb studies are more difficult to perform and thus limited in number. Two studies have investigated auditory-cued foot extension flexion in clinically isolated syndrome (CIS) (Filippi et al., 2004) or primary progressive MS (Ciccarelli et al., 2006) and found increased brain activation. A recent study investigating lower limb position sense in early relapsing–remitting MS (RRMS) demonstrated functional activation changes with unchanged ipsilateral proprioception performance, suggesting potential cortical reorganisation to perform correctly (Iandolo et al., 2020). Thus, little is known about brain activity changes in MS during a complex lower limb motor control that could contribute to loss of mobility and falls, and there are to the best of our knowledge, no studies to date that directly compare upper and lower limb motor control using an identical task, so potential neurophysiological differences contributing to the differential progression of upper and lower limb disabilities remain poorly understood.

This study aimed to compare brain activations associated with the performance of a complex motor control task with the hand or foot between healthy control (HC) subjects and pwMS with minimal clinical disability. We hypothesised that, in the absence of overt clinical impairments, patients would nonetheless display deficits in the upper and lower limb motor control that would be associated with altered functional brain activity. Moreover, as is evident clinically in pwMS, we expected to observe differences in the degree of functional impairment between upper and lower limbs that would be associated with differences in the degree of activation differences between controls and patients. The motor task involved a controlled visually guided contraction of the ankle dorsiflexors (tibialis anterior) or finger/thumb flexors muscles (Mayhew, Porcaro, Tecchio, & Bagshaw, 2017; Shanahan, Hodges, Wrigley, Bennell, & Farrell, 2015), chosen to activate a broad network involved in integrating complex proprioceptive and visual inputs to accurately track a moving target. In addition, we used ultra-high field 7 Tesla (7T) MRI to perform simultaneous multi-slice fMRI at near anatomical MRI resolution (1.24 mm isotropic) with high temporal resolution (1.7 s) resulting in higher accuracy and sensitivity (Hale et al., 2010) to detect subtle and focal activation differences between groups that are potentially undetectable by clinical field strength imaging systems.

2 | METHODS

2.1 | Participants

Twenty-eight participants with RRMS (mean age = 41.9 ± 10.0 years; 23 women) were recruited from the Royal Melbourne Hospital, Melbourne, Australia. Inclusion criteria at time of recruitment were: diagnosis with clinically definite MS according to the revised 2010 McDonald criteria (Polman et al., 2011), no relapses during the 6 months prior and no to minimal clinical disability, that is, Expanded Disability Status Scale (EDSS) < 4, and Kurtzke Functional Systems

Scale (FSS) for pyramidal and cerebellar function ≤ 2 (Kurtzke, 1983). Exclusion criteria were: any neurological condition other than MS, orthopaedic conditions causing disability of the lower limbs (including painful osteoarthritis), and coexisting cardiovascular disease. Seventeen HC (mean age = 39.3 ± 7.3 years; 10 women) with no reported history of neurological disorders were recruited for comparisons. PwMS received standard of care, were on disease modifying treatments and did not undergo a relapse at least 6 months prior testing. No treatment information was recorded for a single patient. Approval was obtained from the Melbourne Health Human Research Ethics Committee and all participants provided a voluntary written consent prior to participation.

2.2 | MRI acquisition

Image acquisition was conducted using a whole body Magnetom 7T MRI system (Siemens Healthcare, Erlangen, Germany) with a single-channel transmit and 32-channel receive head coil (Nova Medical, Wilmington, MA). Two runs of fMRI were acquired (upper and lower limb motor tasks performed in separate runs) with the following parameters: repetition time (TR) = 1,700 ms; echo time (TE) = 34.4 ms; flip angle (FA) = 65° ; multiband slice acceleration factor = 6; fat suppression; GRAPPA phase acceleration factor = 2; 120 slices; 1.24 mm isotropic resolution; 165 volumes; image matrix = 168×168 (Moeller et al., 2010). In addition, a three-dimensional T1-weighted structural image (MP2RAGE: TR = 4,900 ms; TE = 2.89 ms; inversion time (TI) = 700/2,700 ms; FA = $5/6^\circ$; 192 slices; GRAPPA phase acceleration factor = 4; phase encoding direction = AP; voxel size = 0.9 mm isotropic; image matrix = 256×256) was used for brain volumetric measurements. A fluid-attenuated inversion recovery (FLAIR) scan was acquired for lesion identification (TR = 10,000 ms; TE = 96 ms; TI = 2,600 ms; FA = 145° ; 45 axial slices; GRAPPA phase acceleration factor = 3; voxel size = $1.2 \times 1.2 \times 3.0$ mm, image matrix = 192×192).

2.3 | Anatomical MRI processing

Anatomical MRI processing involved lesion detection and brain segmentation. White matter (WM) lesions were detected and marked on the MP2RAGE image using a semi-automated thresholding technique in MRICron (<https://www.nitrc.org/projects/mricron>) with the FLAIR image used as a reference to avoid inclusion of CSF. Next, lesion maps were used to lesion fill the MP2RAGE images using SLF software (<http://atc.udg.edu/nic/slfToolbox/index.html>) in Statistical Parametric Mapping (SPM, version 8), which were subsequently used as input for brain segmentation analyses using FreeSurfer version 6.0-patch (<https://surfer.nmr.mgh.harvard.edu>). From FreeSurfer analysis, the total WM, cortical grey matter, deep grey matter and ventricular volumes were used for statistical analysis and normalised by total intracranial volume. We chose to also include spinal cord cross-sectional area as an important marker of spinal cord damage that could affect

motor control. Spinal cord cross-sectional area at the level of the superior margin of the odontoid peg was marked manually and measured on MP2RAGE images using Horos (v4.0, www.horosproject.org) (Supplementary Figure 1).

2.4 | Pre-MRI testing

Immediately prior to the MRI scan session, the upper and lower limb tasks were explained and practiced in a room outside the 7T scanner using a similar experimental setup as in the scanner. During this practice session, the maximum voluntary contraction (MVC) was performed to tailor contraction intensity to each participant's strength. The participants were asked to squeeze a sphygmomanometer cuff, used to measure force production, with their fingers or by isometric dorsiflexion against a constraint of their foot as strongly as possible for several seconds. All participants performed the task once at a maximum of 5% of MVC as it was found to activate the movement related network activation with minimal head motion (Shanahan et al., 2015).

2.5 | Force matching task participant and apparatus setup

Participants performed a visually guided force-matching task adapted from a previous study and using same apparatus (Shanahan et al., 2015). A flowchart showing connectivity of the various apparatus used in the experiment is shown in Supplementary Figure 2. Setup of the participant in the scanner for upper limb task was that the cuff was held in the right hand between the thumb and fingers with the hand resting on the chest for support and to limit head movement (Figure 1). The lower limb task setup involved the following: the participant's right thigh was supported by the scanner bed, lower leg supported by a pillow and the plantar surface of foot resting against the footplate of an MRI compatible rig, all to restrict movement around the ankle with minimal head motion. A sphygmomanometer cuff was positioned over the dorsum of the right foot as close as possible to the metatarsal heads without covering the toes (Figure 1). Between the upper and lower limb fMRI runs, an experimenter entered the MRI room and removed the cuff from the participant's right hand and positioned it over the foot. The hand run always preceded the foot run in order to minimise repositioning of the subject between runs when removing the cuff from the foot, which we found to cause head movement.

2.6 | Visually guided force-matching motor task

The task involved a controlled, low force contraction of either the right ankle dorsiflexors (tibialis anterior) or the right finger/thumb flexor (hand) muscles in independent fMRI runs (Figure 1). Task design involved 4 (45 s) contraction blocks interleaved with 5 (27 s) periods of rest. During the contraction block, the force target moved up and

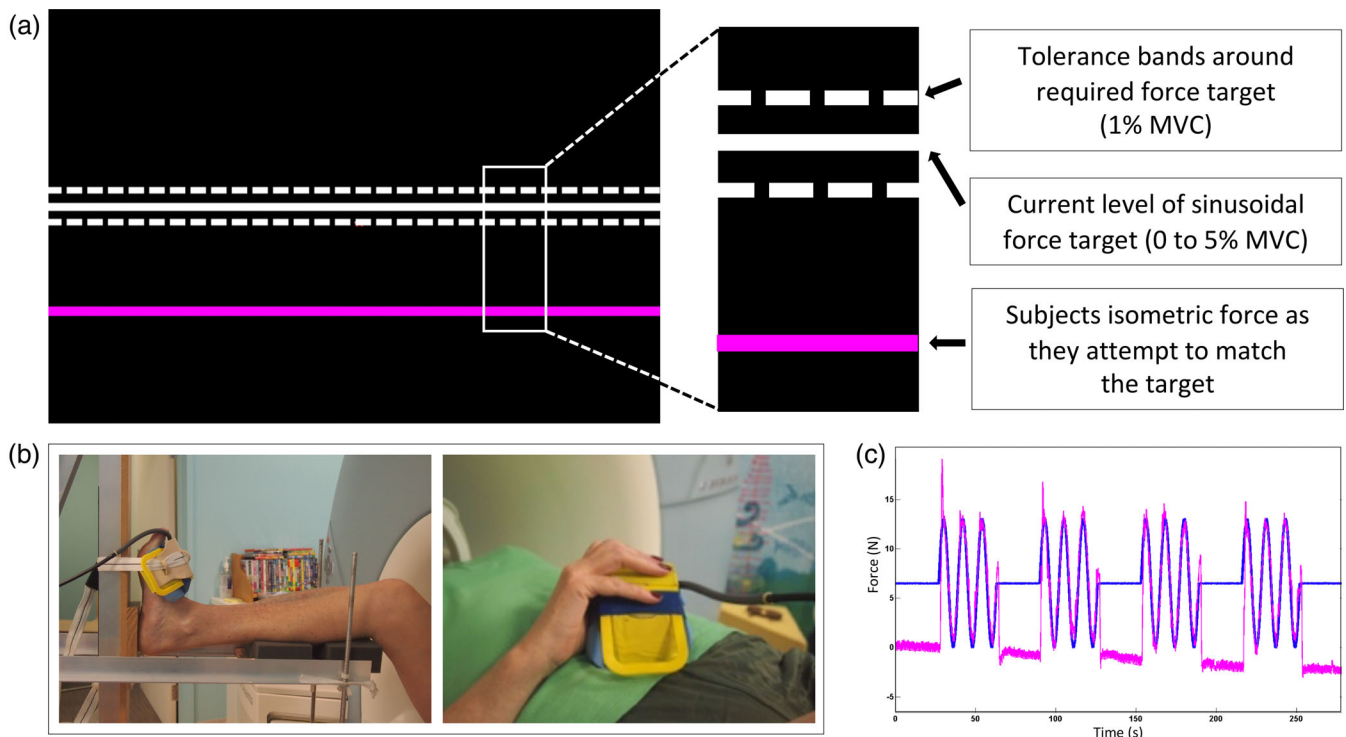


FIGURE 1 Force-matching task during functional MRI acquisition. (a) The task presented to the participants. The white line slowly moved up and down during a task block and the participants were asked to follow the white line as accurately as possible with the pink by squeezing and releasing their fingers or pulling their foot up and down to make the pink line hit the white line. (b) The MR compatible rig used to stabilise the foot and lower leg during the ankle motor task, that is, ankle dorsiflexion to match a force indicator displayed to the participant, is shown on the left. The sphygmomanometer cuff was either positioned over the dorsum of foot close as possible to metatarsal heads without covering toes or held in the right hand between the thumb and fingers (shown on the right image). (c) The blue line reflects the force in four contraction blocks interleaved with five periods of rest. The pink line is an example of the force produced by the participant to match the force indicator displayed on the black screen (white line)

down in a simple harmonic motion with a frequency of 0.125 Hz indicating a target contraction intensity from 0 to 5% of MVC. Participants were instructed to match the sinusoidal target force as accurately as possible. The onset of each contraction block was initiated by an MRI trigger to ensure accurate timing between the experiment and MRI data collection. Both target force and the force produced by the participant were displayed (Figure 1) at the rear of the scanner bore using an LCD projector and viewed through a head-coil mounted mirror. During the rest block, the target force did not move, and participants were asked to relax completely with their eyes open.

2.7 | Upper and lower limb behavioural task parameters

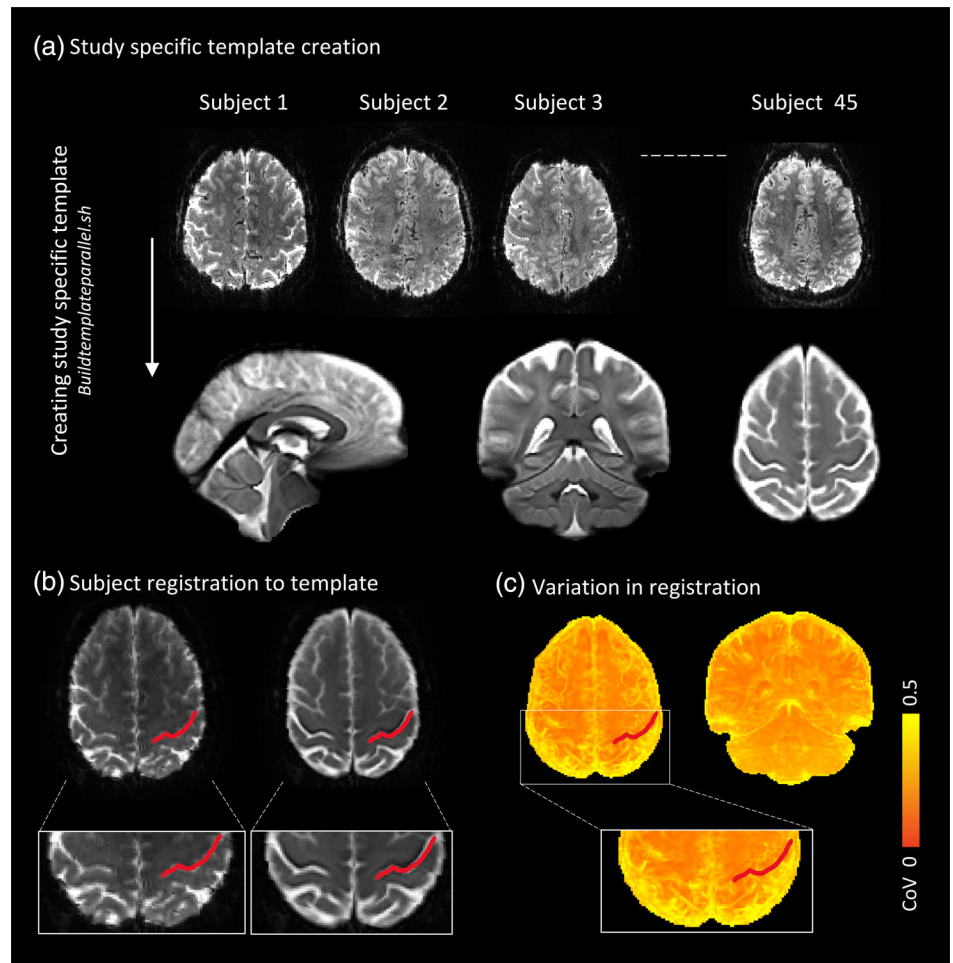
Two behavioural task parameters (lag and error) were computed from the force data acquired during MRI testing using a custom MATLAB script. Lag was defined as the delay between the task cue and the response produced by the participants. Lag was calculated as the maximum cross-correlation between the cue and response time series, expressed in milliseconds (ms). The error was corrected for MVC and

lag and was defined as the root mean square difference between the cue and the lag-corrected response time series, expressed in Newtons (N). The root mean square error is commonly used to calculate the overall difference of measured signal (tracking) from an ideal signal (stimulus waveform).

2.8 | fMRI pre-processing

Due to the cortical specificity and detailed activation patterns evident at 7T, we chose to create a study-specific template script using Advanced Neuroimaging Tool (ANTs, v.2.3.1, <http://stnava.github.io/ANTs/>) (Figure 2). Using 7T imaging and simultaneous multi-slice imaging allowed us to collect fMRI data at near anatomical resolution (1.25 mm isotropic). Therefore, to avoid an unnecessary registration step and therefore avoid additional registration error, we chose to make a template directly from the fMRI data. This also allowed us to identify brain regions in the template that were affected by magnetic field distortions and signal loss (i.e., inferior temporal and orbitofrontal cortices) and to interpret our statistical maps in terms of these distortions. The template creation involves four iterative co-registrations of an example fMRI volume from each participant (HC and MS). Each

FIGURE 2 Study-specific template creation and functional MRI (fMRI) processing steps. (a) A study-specific template was created using Advanced Neuroimaging Tools (v.2.3.1, <http://stnava.github.io/ANTs/>) buildtemplateparallel script and involved four iterative co-registrations of an example fMRI volume from each participant (45 participants in total). (b) An example of a participant to template registration with the red line indicating the central sulcus. (c) The accuracy of template registrations of all subjects is visualised here. The coefficient of variations (CoV) of the fourth iteration was calculated with yellow reflecting high variability between participants, and towards orange more accurate overlap in registrations



co-registration iteration involved rigid body ($n = 20$), affine ($n = 50$) and deformable non-linear ($n = 20$) co-registration calculations followed by averaging of the resultant warped images to create an updated target template. The final template was linearly registered to MNI-152 space for use in fMRI results overlays and coordinate reporting.

fMRI data were pre-processed with the following procedures using FEAT (FSL, FMRIB, Oxford, UK, v.6.0.3): rigid body head motion correction (FMRIB Linear Registration Tool), high pass filtering (cut off 100 s) and nonlinear spatial smoothing (SUSAN, extent threshold 2.5 mm) (Figure 2). Volumes affected by excessive motion (mean relative displacement from previous volume > 0.5 mm) were censored from subsequent analyses. The number of volumes deleted during lower and upper limb movements did not differ between HC (average upper = 4.2, lower = 4.5) and pwMS (average upper = 3.0, lower = 3.4).

2.9 | fMRI statistical analyses

We performed a three-level analysis (run, subject, group) using FEAT, model-based fMRI data toolbox based on general linear modelling. For each subject, two run level analyses were performed (upper limb and lower limb task) including three translation and three rotational motion parameters as covariates. Two group-level analyses were

performed. First, the main effect of the task was compared between HC and pwMS for upper and lower limbs separately including hand dominance as covariate as it could potentially influence the fMRI signal. Where significant clusters were detected, post hoc correlations were performed in SPSS to investigate the relationship between the max z-stat values extracted from the clusters (using fsfstats from the FSL software library) and task performance (lag and force error), volumetrics using and clinical disability (EDSS) using partial (rank) correlation, including hand dominance, sex and age as covariates. To contextualise the effects of hand dominance, the group analyses were repeated without hand dominance as a covariate.

Second, differences in activation associated specifically with upper or lower limb task performance were investigated. For each participant, subject level analyses were performed on unthresholded run-level activation maps to calculate activation maps specific to either upper or lower limb movements using the following contrasts: upper $>$ lower and lower $>$ upper. Higher level analyses including hand dominance as covariate were subsequently performed to calculate significant mean activation maps for upper and lower limbs specifically, and to compare these activation patterns between groups.

All group level statistical analyses employed FLAME 1 mixed effects analysis, and significant voxels were identified using family wise error correction with a threshold of z-stat > 2.3 and cluster wise

significance of $p < .05$. A mask of the mean activation maps of all participants was created and used for all analyses in post-stats to ensure that only brain regions found to be significantly active during the upper or lower limb tasks were included. Brain regions were identified using the peak coordinates and the intersection between suprathreshold regions of activation and regions of interest contained within the Brainnetome atlas (Fan et al., 2016), cerebellar regions using SUIT (included in FSL 6.0.1, FMRIB 2012, <https://fsl.fmrib.ox.ac.uk/fsl/>) and brainstem regions using Swenson atlas of the brainstem (<https://www.dartmouth.edu/~rswenson/Atlas/BrainStem/index.html>).

2.10 | Statistical analyses

Statistical analyses were performed using SPSS (version 26; IBM Corp., Armonk, NY). Demographics, brain volumetrics and task parameters were compared between HC and pwMS with independent sample t tests, or Mann-Whitney U tests when violations of the

assumption of normality occurred (based on Kolmogorov-Smirnov testing and histogram inspection). Partial correlations were performed to investigate relations between the lag and force error of the upper limb and lower limb and between upper and lower limb task performance. In addition, partial correlations were performance between task performance measures, brain volumetrics and clinical disability. If non-normally distributed, partial rank correlations were performed. For all correlation analyses, age, sex and hand dominance were included as covariates. p -values were corrected using false discovery rate and were considered statistically significant $< .05$.

3 | RESULTS

3.1 | Demographics and clinical characteristics

The demographics, clinical measures and brain and lesion volumes are presented in Table 1. PwMS were all diagnosed with RRMS and had a

TABLE 1 Demographic, clinical, MRI and task performance characteristics

	Healthy controls (n = 17)	MS patients (n = 28)	p -value	p -value FDR_{correc}
Demographics				
Sex, F/M ^a	10/7	23/5	.086	.151
Age	39.29 (7.34)	41.75 (10.01)	.385	.415
Disease duration		6.50 (3.94)		
Dominant hand, R/L ^a	14/3	27/1	.108	.168
MVC hand	74.14 (16.53)	61.09 (13.51)	.006	.014 ^b
MVC foot	73.80 (18.71)	51.69 (20.42)	.001	.014 ^b
Disability scores				
EDSS ^c		1.5 (1.0, 1.5)		
Pyramidal FSS ^c		1.0 (0.0, 1.0)		
Cerebellar FSS ^c		0.0 (0.0, 1.0)		
Volumetric data				
WMV ^d , % ICV	33.48 (3.78)	29.74 (3.70) ^b	.002 ^b	.007 ^b
CGMV ^d , % ICV	31.55 (3.09)	29.45 (2.30) ^b	.014 ^b	.028 ^b
DGMV ^d , % ICV	5.94 (0.81)	5.29 (0.64) ^b	.005 ^b	.014 ^b
Ventricles ^d , % ICV	2.06 (1.17)	2.65 (1.28) ^b	.130	.182
Lesion volume, log mm ³		3.10 (0.64)		
Spinal cord C1/C2 CSA, mm ²	69.81 (6.82)	70.71 (10.27)	.752	.752
Task parameters				
Upper limb lag, ms	184.71 (113.75)	216.07 (90.08)	.201	.256
Upper limb force error, N	0.31 (0.07)	0.34 (0.10)	.296	.345
Lower limb lag, ms	142.35 (116.49)	266.43 (120.68) ^b	.002 ^b	.009 ^b
Lower limb force error, N	0.30 (0.05)	0.45 (0.16) ^b	.001 ^b	.007 ^b

Note: All variables were tested using independent samples t test and values represent means and SDs unless denotes otherwise.

Abbreviations: CGMV, cortical grey matter volume; DGMV, deep grey matter volume; EDSS, Expanded Disability Status Scale; F, females; FDR, false discovery rate; FSS, Functional System Score; ICV, intracranial volume; L, left; M, males; MS, multiple sclerosis; MVC, maximum voluntary contraction; R, right; WMV, white matter volume.

^aChi-square test.

^bSignificant difference between people with multiple sclerosis and healthy controls at $p < .05$.

^cMedian and interquartile range.

^dBrain volumes were normalised for intracranial volume.

mean disease duration of 6.4 years ($SD = 3.9$), median EDSS of 1.5 (interquartile range = 1, 1.5). No differences between groups were observed for age, sex or hand dominance. Compared to HC, pwMS displayed significantly reduced WM volume ($p = .002$), cortical grey matter volume ($p = .014$) and deep grey matter volume ($p = .005$). No differences were observed for ventricular volume and spinal cord cross-sectional area.

3.2 | Motor task performance

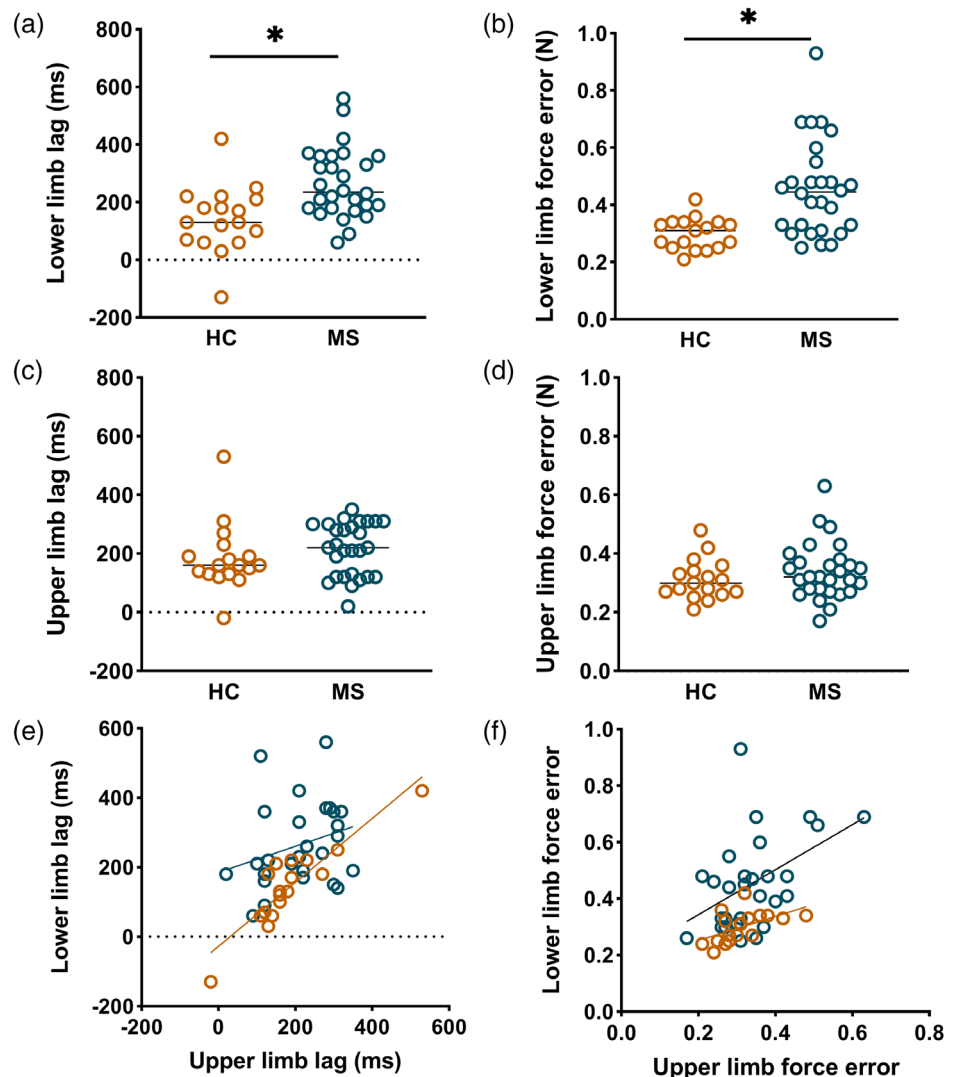
PwMS displayed lower hand (-13.05 N, $U = 132.00$, $p = .013$) and foot (-22.11 N, $t(43) = -3.63$, $p = .001$) MVC and a higher force error ($+0.15$ N, $U = 91.00$, $p = .001$) and a longer lag ($+124$ s, $t(43) = -3.39$, $p = .002$) during the lower limb task but not during the upper limb task (Table 1, Figure 3). In both pwMS and HC, no correlations between force error and lag were found for either upper or lower limbs. Upper and lower limb force error did significantly correlate in pwMS ($p = .028$, $r = .440$), but not in HC ($p = .351$, $r = .270$). Upper limb lag

was significantly associated with lower limb lag in HC only ($p < .001$, $r = .902$), but not in pwMS ($p = .332$, $r = .202$) (Figure 3). No correlations were observed between task parameters (lag and force error) and EDSS.

3.3 | Disease related functional activation changes

Main patterns of activation are shown in Figure 4. During the lower limb task, pwMS displayed reduced activation in three ipsilateral (right) cerebellar clusters including I-IV, V, VI, Crus I/II, (Vermis) VI and brainstem, compared to controls (Figure 5, Table 2). In addition, reduced activation was observed in three ipsilateral (right) cerebrum clusters within the superior parietal lobule (Brodmann area (BA) 7 [objects in space in relation to body] and BA 5 [somatosensory processes and movement]), inferior temporal gyrus (BA 37 [processing colour, face/body recognition], BA 39 [body image] and V5/MT+ [visual motion]) and inferior occipital gyrus [object recognition, BA 37, V5/MT+] in pwMS compared to HC (Figure 5, Table 2). During

FIGURE 3 The functional force tracking task parameters. These plots demonstrate the group differences in task performance (lag and force error) and the correlations between the upper and lower limb performance. Each circle reflects a participant, and the healthy controls (HC) are visualised in orange and people with multiple sclerosis (MS) in blue. (a,b) People with MS showed significantly longer lag ($+124$ s, $p = .002$) and higher force error ($+0.15$ N, $p = .001$) during lower limb force tracking, compared to HC. (c,d) No differences in performance were observed during upper limb movements. (e,f) Upper and lower limb lag correlated significantly in HC ($p < .001$, $r = .902$), but not in MS ($p = .322$, $r = .202$). Force error of the upper and lower limb did significantly correlate in MS ($p = .028$, $r = .440$), but not in HC ($p = .351$, $r = .270$). Excluding positive and negative outliers in HC (lower limb and upper limb lag) and MS patients (lower limb force error) gave similar results and changed p -values minimally



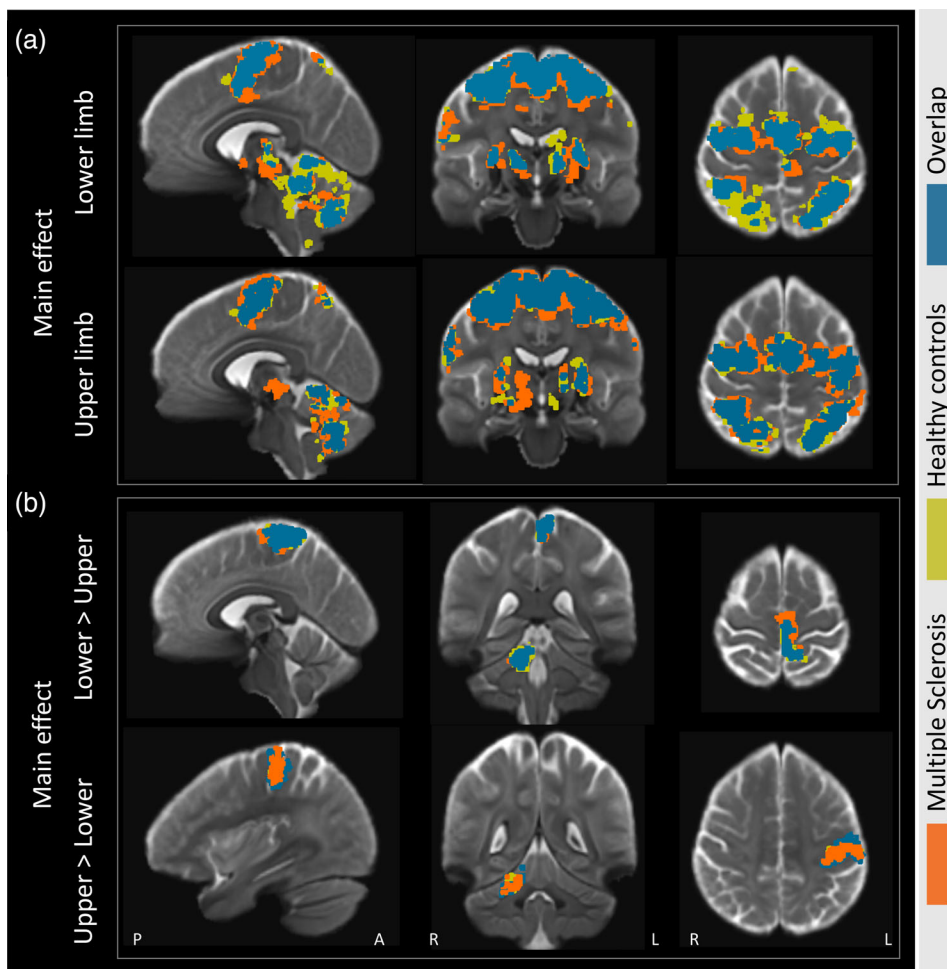


FIGURE 4 Average activation maps. (a) The mean activation maps during the upper and lower limb visually guided force-matching tasks. (b) Activation patterns specifically related to either lower limb (lower > upper) or upper limb (upper > lower) movements. The main effects for healthy controls (mustard yellow) and people with multiple sclerosis (orange) are presented in an overlaid manner with the overlap between groups presented in petroleum blue

the upper limb task, reduced activation was observed within the inferior occipital gyrus (visual processing area) in pwMS compared to controls.

Several significant post hoc correlations were identified between peak z-stat values extracted from significant clusters and task performance variables, lesion volume and EDSS (Figure 5). Lesion volume correlated negatively with peak z-stat values from the clusters within inferior temporal gyrus (BA 37, BA 39 and V5/MT+) ($r = -.476$, $p = .019$), superior parietal lobule (BA 5 and 7) ($r = -.460$, $p = .024$) and brainstem and cerebellar right I–IV and V ($r = -.474$, $p = .019$). A negative relation was found between clinical disability (EDSS) and peak z-stat values from the brainstem and cerebellar right I–IV and V cluster ($r = -.417$, $p = .034$). Lower limb force error correlated positively with the inferior occipital gyrus (V5/MT+ and BA 37) cluster peak z-stat values ($r = .541$, $p = .006$).

We observed a range of moderate correlations between brain volumetrics, motor performance and clinical disability (Supplementary Table 1).

Group analysis without hand dominance included as covariate resulted in lower cerebellar Crus I/II activation and increased cortical M1/premotor activation during lower limb movements, but no significant change was observed during upper force tracking (Supplementary Figure 3).

3.4 | Activation patterns related to upper and lower limb movements specifically

In both pwMS and HC activity specific to lower limb movements was observed in the contralateral medial primary somatosensory cortex and M1, whereas activation patterns related to upper limb movements were observed in lateral precentral gyrus, consistent with known somatotopy. Within the cerebellum, activity specific to upper limb movements was seen largely in the ipsilateral V–VI and lower limb activation was observed in the ipsilateral I–IV. Activation within the primary sensorimotor cortices and cerebellum largely overlapped and were not significantly different between group (Figure 4).

4 | DISCUSSION

In the present study, we aimed to investigate the complex upper and lower limb motor control in pwMS with minimal sensorimotor impairments using ultra-high field fMRI and a visually guided force-matching task. We found that pwMS displayed altered task performance and reduced activation of several regions within the cerebellum (I–IV, V, VI, Crus I/II), occipital and superior parietal cortices during lower limb movements, compared to HC, with the level of activation related to

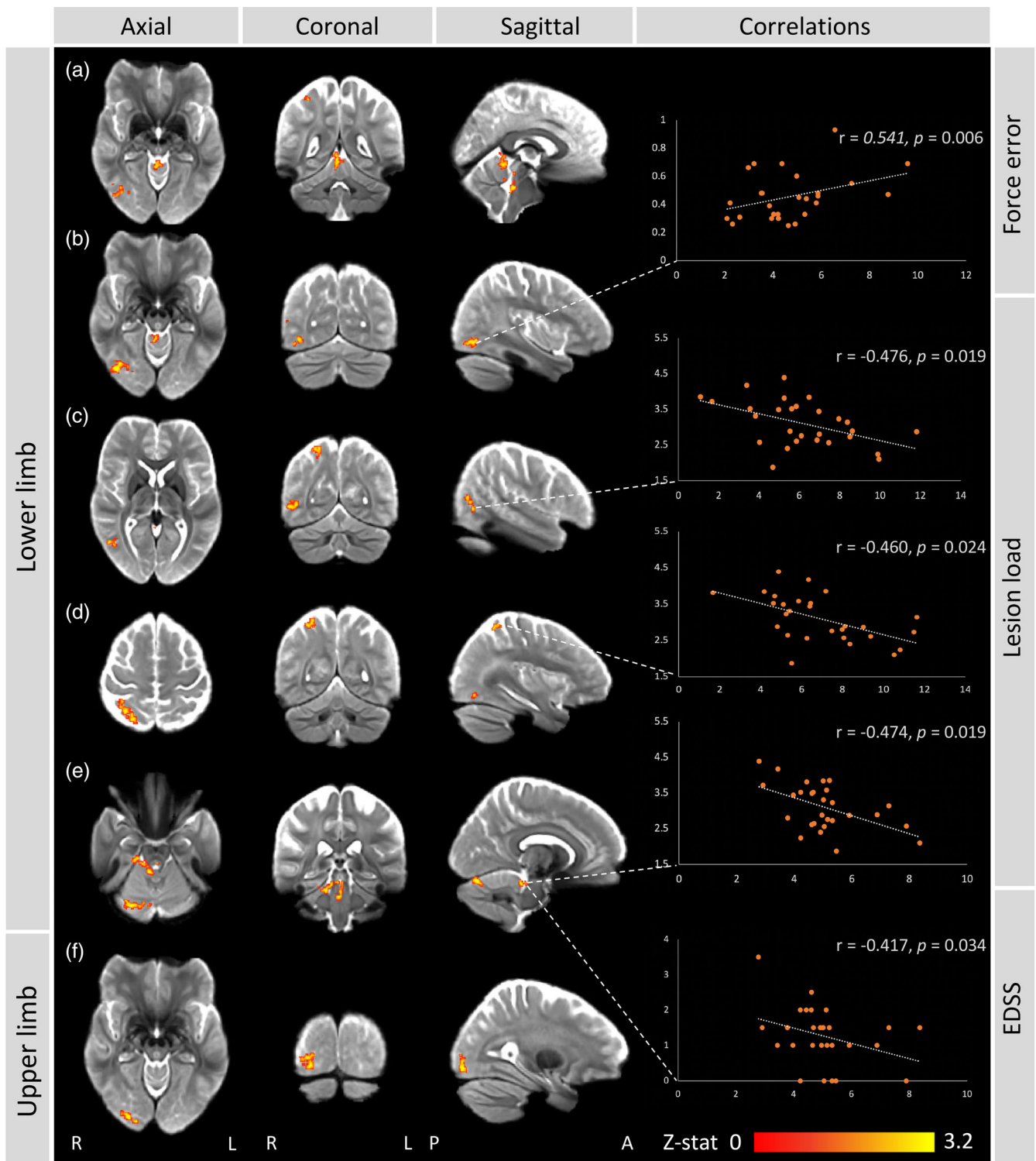


FIGURE 5 Functional brain activity changes in minimally disabled people with multiple sclerosis. (a-e) During the lower limb force-matching task, compared to healthy controls, people with multiple sclerosis (pwMS) displayed hypoactivation within several clusters located in right: (a) cerebellum (I-IV), (b) inferior occipital gyrus (V5/MT+ and Brodmann area (BA) 37), (c) inferior temporal gyrus (V5/MT+, BA 37 and 39), (d) superior parietal lobule (BA 5 and 7), (e) cerebellum (I-IV, VI, Vermis VI, Crus I/II) and brainstem (anterior of fourth ventricle). Correlations were found with lower limb force error, lesion load and Expanded Disability Status Scale (EDSS) scores. (f) During upper limb force tracking, pwMS displayed lower brain activity within the inferior occipital cortex, compared to controls. Maximum z-stat values are plotted on the x-axis and variables of interest (EDSS, lesion load, task performance) on the y-axis

TABLE 2 MNI coordinates and anatomical description

Description anatomical regions (peak and overlap)	Peak MNI coordinates		
	X	Y	Z
Lower limb movements (MS < HC)			
Rostral area 7 (superior parietal lobule)	23.84	-60.04	61.01
Intraparietal area 7 (superior parietal lobule)			
Lateral area 5 (superior parietal lobule)			
Caudal area 7 (superior parietal lobule)			
Ventrolateral area 37 (inferior temporal gyrus)	52.87	-63.98	-1.56
V5/MT+ (lateral occipital cortex)			
Dorsolateral area 37 (middle temporal gyrus)			
Ventrolateral area 37 (inferior temporal gyrus)			
Rostradorsal area 39 (inferior parietal lobule)			
Inferior occipital gyrus (lateral occipital cortex)	40.30	-79.71	-12.83
V5/MT+ (lateral occipital cortex)			
Lateroventral area 37 (fusiform gyrus)			
Medioventral area 37 (fusiform gyrus)			
Cerebellar right I-IV	2.81	-44.55	-3.50
Left I-IV			
Cerebellar right VI	7.66	-79.77	-19.06
Right Crus I/II			
VI			
Vermis VI			
Brainstem (anterior of fourth ventricle, reticular formation, etc.)	5.88	-37.43	-33.12
Cerebellar right I-IV			
Cerebellar right V			
Medioventral area 37 (fusiform gyrus)			
Upper limb movements (MS < HC)			
Inferior occipital gyrus (lateral occipital cortex)	25.03	-93.81	-10.71
Occipital polar cortex (lateral occipital cortex)			

Note: This table shows the location of the max z-stat of the significant clusters (group differences) in MNI coordinates. Cortical and subcortical regions are localised using the Brainnetome atlas (Fan et al., 2016), cerebellar regions using SUIT (included in FSL 6.0.1, FMRIB 2012, <https://fsl.fmrib.ox.ac.uk/fsl/>) and brainstem regions using Swenson atlas of the brainstem (<https://www.dartmouth.edu/~rswenson/Atlas/BrainStem/index.html>).

Abbreviations: BA, Brodmann area; HC, healthy controls; LL, lower limb; MS, multiple sclerosis; UL, upper limb.

task performance, clinical disability and lesion load. During the upper limb task, motor performance was preserved in pwMS, yet activity within the inferior occipital cortex was lower compared to controls.

4.1 | Lower limb functional activation changes

We detected several small loci with reduced activation within the cerebrum and cerebellum during a visually guided force matching in pwMS, compared to HCs. Activation changes were associated with lower limb force error, a metric of sensorimotor integration, and EDSS scores, suggesting a role of functional disturbances in clinical disability

early in the disease. We observed cortical changes during lower limb movements in visual-motor regions including BA 5 and 7, involved in somatosensory association processes including visuomotor attention and location of objects in space (integration proprioception and vision), as well as during foot and hand movements in the occipital cortex including BA 37, occipital pole (primary visual processes) and middle temporal visual area (processing of motion). Reduced activation was observed in the occipital during upper limb movement as well. Unexpectedly this was the only identified difference during the upper limb force tracking and potentially reflects differences in visual attention required to maintain tracking. In addition to cortical changes, we observed reduced cerebellar Crus I/II and cerebellar I-IV, V and VI

activation during lower limb force tracking. Cerebellar Crus I/II are suggested to be primarily involved in higher-level cognitive processes. These regions are included in cerebral networks involving cognitive control (Buckner, Krienen, Castellanos, Diaz, & Yeo, 2011) and activation within Crus I/II was reported higher during a cognitive compared to a motor task (Stoodley, Valera, & Schmahmann, 2012). Besides cognitive control, lesions in these regions have been associated with worse motor task performance in stroke patients (Stoodley, MacMore, Makris, Sherman, & Schmahmann, 2016). Cerebellar I–IV and VI are suggested to be primarily involved in sensorimotor processes. Lobule IV and VI, along with V VIII B map to the somatosensory cerebral network encompassing hand and foot representations (Buckner et al., 2011). Overall, the areas implicated by our study include both sensorimotor and visual-motor regions, and activation changes were associated with lower limb force error, together suggesting that motor control impairments in MS are related to dysfunctions in visuomotor integration.

This is one of the first studies to use a complex motor control task in MS (Boonstra et al., 2018; Boonstra et al., 2019). Previous functional task imaging studies have used simple motor tasks such as finger tapping (Filippi et al., 2004; Lee et al., 2000; Mezzapesa et al., 2008; Reddy et al., 2000; Rocca et al., 2003, 2005) and foot flexion and extension or increased complexity by performing a task with both hand and foot (Filippi et al., 2004). Using simple motor tasks resulted in increased activation in motor regions such as M1 (Filippi et al., 2004; Lee et al., 2000; Reddy et al., 2000, 2002; Rocca et al., 2005), often interpreted to be a compensatory mechanism in response to the pathological damage, and reduced cerebellar activation in patients with worse disability (Ciccarelli et al., 2006) and over time (Pantano et al., 2005). To determine whether changes in activation are adaptive or maladaptive and are predictive of progressive decline would require longer term follow-up that was outside the scope of the current study. In contrast to more simple tasks, increasing complexity resulted in more widespread activation in supplementary motor area, thalamus, and frontal regions. Compared to controls, CIS patients displayed cortical and subcortical activity changes, but no cerebellar differences (Filippi et al., 2004), potentially due to clinical field strength used. Imaging at higher field strengths and a task involving complex motor control revealed more subtle deficits in early stages, providing markers for early motor progression.

4.2 | Pathological factors influencing lower limb functional impairments

The aim of this study was to investigate functional mechanisms underlying impairments in movements, so we did not undertake detailed structural investigations. However, we did identify gross atrophy of cortical and deep grey matter and WM and the extend of cortical and cerebellar activation was negatively correlated with the lesion load, that is, the higher the lesion volume the lower the brain activity. These results suggest that structural damage within the brain could explain activation and behaviour changes observed during lower limb

movements specifically. Besides the thalamus and precentral gyrus (M1), areas important in motor control, the cerebellum is one of the first regions to become atrophic in relapse-onset disease (Eshaghi et al., 2018), possibly affecting brain function. The cortical regions on the other hand were not within the somatotopically mapped lower limb regions identified in the lower > upper contrast, but in visuomotor integration areas and therefore cannot be attributable to reduced sensory input or motor output to lumbar spinal cord motor neurons. In addition, we did not observe differences in cervical spinal cord cross-sectional area between patients and controls. We were unable to fully characterise cervical cord lesions due to the limited field of view afforded by the use of a transmit/receive head coil necessary for 7T imaging. However, lesions are primarily observed in the cervical spinal cord (59%) (Weier et al., 2012), clearly affecting both upper and lower limb function and early MS spinal cord lesions are often asymptomatic (Granella et al., 2019) and do not predict disability progression (Dekker et al., 2017).

4.3 | Lower and upper limb performance in pwMS with minimal impairments: Different processes?

In our study using a motor control task we were able to differentiate between upper and lower limb performance and brain activity. PwMS displayed delayed and more erroneous force tracking compared to HC for lower but not upper limbs. Whereas during upper limb force tracking only a single region differed between groups, multiple clusters were observed during lower limb movements in pwMS. These lower limb changes were also clinically meaningful as activation correlated significantly with markers of clinical disability including EDSS severity and lesion load, these associations were not found with upper limb activation. Together, this suggests that, at least in part, divergent pathological processes drive progression of upper and lower limb impairments. This interpretation is supported by a previous study showing only a moderate correlation between a hand-to-mouth task and walking revealed using advanced kinematic analyses (Coghe et al., 2019). Also, clinical observations of pwMS often report impairments in lower limb function early in the disease (Benedetti et al., 1999; Kister et al., 2013; Martin et al., 2006). Potentially, lower limb impairments precede upper limb disability, which would require a longitudinal design to investigate.

4.4 | Force-matching for studying visuomotor integration in pwMS

Here, we used a force matching task to elicit submaximal contractions of the tibialis anterior (lower limb task) or hand flexion (upper limb task) performed in separate runs adapted from a study (Shanahan et al., 2015). With this task, we aimed to model not only basic sensorimotor behaviour, but complex motor control behaviours required for daily life. Similar tasks have been used previously to study the basic neurophysiology involved in visuomotor control (Keisker, Hepp-Reymond,

Blickenstorfer, & Kollias, 2010; Mayhew et al., 2017), showing that visual feedback resulted in stronger activation, that scaled with MVC. Stronger correlations were found between activation and behavioural performance when participants performed low MVC contractions (10%), potentially due to greater neuronal recruitment required for finer motor control. We used an MVC of 5% that was selected to both increase the difficulty of the task, and to minimise head motion, resulting in the activation of a broad network of visual and oculomotor, premotor and motor areas. We conclude that force-matching tasks provide a relatively straightforward means to investigate complex visuomotor integration.

4.5 | Methodological considerations and limitations

In this study, we used ultra-high field MRI with the goal of detecting more specific activation loci with better accuracy due to high sensitivity. For low-resolution fMRI data, large spatial smoothing kernels are commonly used to enhance signal-to-noise ratio and to minimise the effects of misregistration. However, this also reduces accuracy as it can lead to incorrect estimation of true spatial localisation and therefore Type-I error (Heidemann et al., 2012; Sacchet & Knutson, 2013). We therefore chose to create a study-specific template to improve the accuracy of spatial co-registrations and therefore we were able to use very limited smoothing in our data (2.5 mm). To conclude, using ultra-high field and a study-specific template led to identification of detailed activation patterns specific to movement without losing sensitivity.

The comprehensive study design involving both MRI testing and laboratory gait analysis in two different locations resulted in long assessment times and a relatively small sample size. Future studies including a larger sample size would be recommended to confirm findings. Despite the sample size, we used focused inclusion criteria which resulted in a relatively homogeneous group of patients and the motor performance assessments at 7T were sensitive enough to detect subtle changes in brain activity in patients with minimal disabilities. While there are significant advantages for the use of ultra-high field for fMRI such as higher raw signal to noise ratio (Yoo et al., 2018), stronger susceptibility effects (Ladd et al., 2018), and signal more closely attributable to venules than feeding veins (Cheng, 2018), worse magnetic field inhomogeneities can lead to signal dropout and warping around the inferior temporal and orbitofrontal cortices. For the current study, these areas were not of major interest and the study-specific template demonstrated the very high signal-to-noise ratio across the brain with very little signal loss in areas of interest such as the sensorimotor cortices and cerebellum.

Hand but not foot dominance was recorded during testing. Even though in the majority of people dominance of the hand and foot are similar (Barut, Ozer, Sevinc, Gumus, & Yuntun, 2007), we recommend including both as covariates in future studies as well as the use of validated dominance assessments.

5 | CONCLUSION

These results demonstrate that ultra-high field fMRI during complex hand and foot tracking can identify subtle impairments in movement and brain activity in otherwise minimally impaired pwMS, with differential effects for upper and lower limb impairments. Minimally disabled pwMS displayed altered lower limb movements and brain activation with preserved upper limb function but altered brain activation. Our findings demonstrate an important link between the impaired lower limb motor control and altered neuronal activity within regions related to sensorimotor integration in the parietal cortex and fine motor control in the cerebellum.

ACKNOWLEDGMENTS

The authors would like to thank all the participants and acknowledge the facilities, scientific and technical assistance from the National Imaging Facility, a National Collaborative Research Infrastructure Strategy (NCRIS) capability, at the Melbourne Brain Centre Imaging Unit, The University of Melbourne.

CONFLICT OF INTERESTS

The authors declare no conflict of interest that is directly relevant or directly related to the work described in this manuscript.

DATA AVAILABILITY STATEMENT

Anonymised data are available from the corresponding author upon request.

ORCID

Myrte Strik  <https://orcid.org/0000-0001-8995-9899>

Menno M. Schoonheim  <https://orcid.org/0000-0002-2504-6959>

REFERENCES

- Barut, C., Ozer, C. M., Sevinc, O., Gumus, M., & Yuntun, Z. (2007). Relationships between hand and foot preferences. *International Journal of Neuroscience*, 117(2), 177–185. <https://doi.org/10.1080/00207450600582033>
- Benedetti, M. G., Piperno, R., Simoncini, L., Bonato, P., Tonini, A., & Giannini, S. (1999). Gait abnormalities in minimally impaired multiple sclerosis patients. *Multiple Sclerosis*, 5(5), 363–368. <https://doi.org/10.1177/135245859900500510>
- Boonstra, F. M., Noffs, G., Perera, T., Jokubaitis, V. G., Vogel, A. P., Moffat, B. A., ... Kolbe, S. C. (2019). Functional neuroplasticity in response to cerebello-thalamic injury underpins the clinical presentation of tremor in multiple sclerosis. *Multiple Sclerosis*, 26(6), 696–705. <https://doi.org/10.1177/1352458519837706>
- Boonstra, F. M. C., Perera, T., Noffs, G., Marotta, C., Vogel, A. P., Evans, A. H., ... Kolbe, S. C. (2018). Novel functional MRI task for studying the neural correlates of upper limb tremor. *Frontiers in Neurology*, 9(JUL), 1–7. <https://doi.org/10.3389/fneur.2018.00513>
- Buckner, R. L., Krienen, F. M., Castellanos, A., Diaz, J. C., & Yeo, B. T. T. (2011). The organization of the human cerebellum estimated by intrinsic functional connectivity. *Journal of Neurophysiology*, 106(5), 2322–2345.
- Cheng, K. (2018). Exploration of human visual cortex using high spatial resolution functional magnetic resonance imaging. *NeuroImage*, 164, 4–9. <https://doi.org/10.1016/j.neuroimage.2016.11.018>

- Ciccarelli, O., Toosy, A. T., Marsden, J. F., Wheeler-Kingshott, C. M., Miller, D. H., Matthews, P. M., & Thompson, A. J. (2006). Functional response to active and passive ankle movements with clinical correlations in patients with primary progressive multiple sclerosis. *Journal of Neurology*, 253(7), 882–891. <https://doi.org/10.1007/s00415-006-0125-z>
- Coghe, G., Corona, F., Pilloni, G., Porta, M., Frau, J., Loreface, L., ... Pau, M. (2019). Is there any relationship between upper and lower limb impairments in people with multiple sclerosis? A kinematic quantitative analysis. *Multiple Sclerosis International*, 2019, 1–6. <https://doi.org/10.1155/2019/9149201>
- Dekker, I., Sombekke, M., Witte, B., Geurts, J., Barkhof, F., Uitdehaag, B., ... Wattjes, M. (2017). Asymptomatic spinal cord lesions do not predict the time to disability in patients with early multiple sclerosis. *Multiple Sclerosis Journal*, 23(2s), 153–156. <https://doi.org/10.1177/https>
- Eshaghi, A., Marinescu, R. V., Young, A. L., Firth, N. C., Prados, F., Cardoso, M. J., ... Ciccarelli, O. (2018). Progression of regional grey matter atrophy in multiple sclerosis. *Brain*, 141, 1665–1677. <https://doi.org/10.1093/brain/awy088>
- Fan, L., Li, H., Zhuo, J., Zhang, Y., Wang, J., Chen, L., ... Jiang, T. (2016). The human Brainnetome atlas: A new brain atlas based on connectonal architecture. *Cerebral Cortex*, 26, 3508–3526. <https://doi.org/10.1093/cercor/bhw157>
- Filippi, M., Rocca, M. A., Mezzapesa, D. M., Ghezzi, A., Falini, A., Martinelli, V., ... Comi, G. (2004). Simple and complex movement-associated functional MRI changes in patients at presentation with clinically isolated syndromes suggestive of multiple sclerosis. *Human Brain Mapping*, 21(2), 108–117. <https://doi.org/10.1002/hbm.10160>
- Granella, F., Tsantes, E., Graziuso, S., Bazzurri, V., Crisi, G., & Curti, E. (2019). Spinal cord lesions are frequently asymptomatic in relapsing–remitting multiple sclerosis: A retrospective MRI survey. *Journal of Neurology*, 266(12), 3031–3037. <https://doi.org/10.1007/s00415-019-09526-3>
- Hale, J. R., Brookes, M. J., Hall, E. L., Zumer, J. M., Stevenson, C. M., Francis, S. T., & Morris, P. G. (2010). Comparison of functional connectivity in default mode and sensorimotor networks at 3 and 7T. *Magnetic Resonance Materials in Physics, Biology and Medicine*, 23(5–6), 339–349. <https://link.springer.com/article/10.1007%2Fs10334-010-0220-0>
- Heidemann, R. M., Ivanov, D., Trampel, R., Fasano, F., Meyer, H., Pfeuffer, J., & Turner, R. (2012). Isotropic submillimeter fMRI in the human brain at 7 T: Combining reduced field-of-view imaging and partially parallel acquisitions. *Magnetic Resonance in Medicine*, 68(5), 1506–1516. <https://doi.org/10.1002/mrm.24156>
- Hubbard, E. A., Wetter, N. C., Sutton, B. P., Pilutti, L. A., & Motl, R. W. (2016). Diffusion tensor imaging of the corticospinal tract and walking performance in multiple sclerosis. *Journal of the Neurological Sciences*, 363, 225–231. <https://doi.org/10.1016/j.jns.2016.02.044>
- Iandolo, R., Bommarito, G., Falcitano, L., Schiavi, S., Piaggio, N., Mancardi, G. L., ... Inglese, M. (2020). Position sense deficits at the lower limbs in early multiple sclerosis: Clinical and neural correlates. *Neurorehabilitation and Neural Repair*, 34(3), 260–270. <https://doi.org/10.1177/1545968320902126>
- Johansson, S., Ytterberg, C., Claesson, I. M., Lindberg, J., Hillert, J., Andersson, M., ... Von Koch, L. (2007). High concurrent presence of disability in multiple sclerosis: Associations with perceived health. *Journal of Neurology*, 254(6), 767–773. <https://doi.org/10.1007/s00415-006-0431-5>
- Keisker, B., Hepp-Reymond, M. C., Blickenstorfer, A., & Kollias, S. S. (2010). Differential representation of dynamic and static power grip force in the sensorimotor network. *European Journal of Neuroscience*, 31(8), 1483–1491. <https://doi.org/10.1111/j.1460-9568.2010.07172.x>
- Kerbrat, A., Gros, C., Badji, A., Bannier, E., Galassi, F., Combès, B., ... Cohen-Adad, J. (2020). Multiple sclerosis lesions in motor tracts from brain to cervical cord: Spatial distribution and correlation with disability. *Brain*, 143, 2089–2105. <https://doi.org/10.1093/brain/awaa162>
- Kister, I., Bacon, T. E., Chamot, E., Salter, A. R., Cutter, G. R., Kalina, J. T., & Herbert, J. (2013). Natural history of multiple sclerosis symptoms. *International Journal of MS Care*, 15(3), 146–158. <https://doi.org/10.7224/1537-2073.2012-053>
- Kolasa, M., Hakulinen, U., Brander, A., Hagman, S., Dastidar, P., Elovaara, I., & Sumelahti, M. L. (2019). Diffusion tensor imaging and disability progression in multiple sclerosis: A 4-year follow-up study. *Brain and Behavior*, 9(1), e01194. <https://doi.org/10.1002/brb3.1194>
- Kurtzke, J. F. (1983). Rating neurologic impairment in multiple sclerosis: An expanded disability status scale (EDSS). *Neurology*, 33(11), 1444–1452. <https://doi.org/10.1212/WNL.33.11.1444>
- Ladd, M. E., Bachert, P., Meyerspeer, M., Moser, E., Nagel, A. M., Norris, D. G., ... Zaiss, M. (2018). Pros and cons of ultra-high-field MRI/MRS for human application. *Progress in Nuclear Magnetic Resonance Spectroscopy*, 109, 1–50. <https://doi.org/10.1016/j.pnmrs.2018.06.001>
- Lee, M., Reddy, H., Johansen-Berg, H., Pendlebury, S., Jenkinson, M., Smith, S., ... Matthews, P. M. (2000). The motor cortex shows adaptive functional changes to brain injury from multiple sclerosis. *Annals of Neurology*, 47(5), 606–613. [https://doi.org/10.1002/1531-8249\(200005\)47:5<606::AID-ANA8>3.0.CO;2-L](https://doi.org/10.1002/1531-8249(200005)47:5<606::AID-ANA8>3.0.CO;2-L)
- Martin, C. L., Phillips, B. A., Kilpatrick, T. J., Butzkueven, H., Tubridy, N., McDonald, E., & Galea, M. P. (2006). Gait and balance impairment in early multiple sclerosis in the absence of clinical disability. *Multiple Sclerosis*, 12(5), 620–628 Retrieved from <http://www.ncbi.nlm.nih.gov/pubmed/17086909>
- Mayhew, S. D., Porcaro, C., Tecchio, F., & Bagshaw, A. P. (2017). fMRI characterisation of widespread brain networks relevant for behavioural variability in fine hand motor control with and without visual feedback. *NeuroImage*, 148, 330–342. <https://doi.org/10.1016/j.neuroimage.2017.01.017>
- Mezzapesa, D. M., Rocca, M. A., Rodegher, M., Comi, G., & Filippi, M. (2008). Functional cortical changes of the sensorimotor network are associated with clinical recovery in multiple sclerosis. *Human Brain Mapping*, 29(5), 562–573. <https://doi.org/10.1002/hbm.20418>
- Moeller, S., Yacoub, E., Olman, C. A., Auerbach, E., Strupp, J., Harel, N., & Ugurbil, K. (2010). Multiband multislice GE-EPI at 7 tesla, with 16-fold acceleration using partial parallel imaging with application to high spatial and temporal whole-brain fMRI. *63(5)*, 1144–1153.
- Ozturk, A., Smith, S. A., Gordon-Lipkin, E. M., Harrison, D. M., Shiee, N., Pham, D. L., ... Reich, D. S. (2010). MRI of the corpus callosum in multiple sclerosis: Association with disability. *Multiple Sclerosis*, 16(2), 166–177. <https://doi.org/10.1177/1352458509353649>
- Pantano, P., Mainero, C., Lenzi, D., Caramia, F., Iannetti, G. D., Piattella, M. C., ... Pozzilli, C. (2005). A longitudinal fMRI study on motor activity in patients with multiple sclerosis. *Brain*, 128, 2146–2153. <https://doi.org/10.1093/brain/awh549>
- Polman, C. H., Reingold, S. C., Banwell, B., Clanet, M., Cohen, J. A., Filippi, M., ... Wolinsky, J. S. (2011). Diagnostic criteria for multiple sclerosis: 2010 revisions to the McDonald criteria. *Annals of Neurology*, 69(2), 292–302. <https://doi.org/10.1002/ana.22366>
- Reddy, H., Narayanan, S., Arnoutelis, R., Jenkinson, M., Antel, J., Matthews, P. M., & Arnold, D. L. (2000). Evidence for adaptive functional changes in the cerebral cortex with axonal injury from multiple sclerosis. *Brain*, 11, 2314–2320. <https://doi.org/10.1093/brain/123.11.2314>
- Reddy, H., Narayanan, S., Woolrich, M., Mitsumori, T., Lapierre, Y., Arnold, D. L., & Matthews, P. M. (2002). Functional brain reorganization for hand movement in patients with multiple sclerosis: Defining distinct effects of injury and disability. *Brain*, 125(22), 2646–2657. <https://doi.org/10.1093/brain/awf283>
- Rocca, M. A., Colombo, B., Falini, A., Ghezzi, A., Martinelli, V., Scotti, G., ... Filippi, M. (2005). Cortical adaptation in patients with MS: A cross-sectional

- functional MRI study of disease phenotypes. *Lancet Neurology*, 4(10), 618–626. [https://doi.org/10.1016/S1474-4422\(05\)70171-X](https://doi.org/10.1016/S1474-4422(05)70171-X)
- Rocca, M. A., Gavazzi, C., Mezzapesa, D. M., Falini, A., Colombo, B., Mascalchi, M., ... Filippi, M. (2003). A functional magnetic resonance imaging study of patients with secondary progressive multiple sclerosis. *NeuroImage*, 19(4), 1770–1777. [https://doi.org/10.1016/S1053-8119\(03\)00242-8](https://doi.org/10.1016/S1053-8119(03)00242-8)
- Sacchet, M. D., & Knutson, B. (2013). Spatial smoothing systematically biases the localization of reward-related brain activity. *NeuroImage*, 66, 270–277. <https://doi.org/10.1016/j.neuroimage.2012.10.056>
- Shanahan, C. J., Hodges, P. W., Wrigley, T. V., Bennell, K. L., & Farrell, M. J. (2015). Organisation of the motor cortex differs between people with and without knee osteoarthritis. *Arthritis Research and Therapy*, 17(1), 164. <https://doi.org/10.1186/s13075-015-0676-4>
- Souza, A., Kelleher, A., Cooper, R., Cooper, R. A., Iezzoni, L. I., & Collins, D. M. (2010). Multiple sclerosis and mobility-related assistive technology: Systematic review of literature. *Journal of Rehabilitation Research and Development*, 47(3), 213–224. <https://doi.org/10.1682/JRRD.2009.07.0096>
- Stoodley, C. J., MacMore, J. P., Makris, N., Sherman, J. C., & Schmahmann, J. D. (2016). Location of lesion determines motor vs. cognitive consequences in patients with cerebellar stroke. *NeuroImage: Clinical*, 12, 765–775. <https://doi.org/10.1016/j.nicl.2016.10.013>
- Stoodley, C. J., Valera, E. M., & Schmahmann, J. D. (2012). Functional topography of the cerebellum for motor and cognitive tasks: An fMRI study. *NeuroImage*, 59(2), 1560–1570. <https://doi.org/10.1016/j.neuroimage.2011.08.065>
- Weier, K., Mazraeh, J., Naegelin, Y., Thoeni, A., Hirsch, J. G., Fabbro, T., ... Gass, A. (2012). Biplanar MRI for the assessment of the spinal cord in multiple sclerosis. *Multiple Sclerosis Journal*, 18(11), 1560–1569. <https://doi.org/10.1177/1352458512442754>
- Yoo, P. E., John, S. E., Farquharson, S., Cleary, J. O., Wong, Y. T., Ng, A., ... Moffat, B. A. (2018). 7T-fMRI: Faster temporal resolution yields optimal BOLD sensitivity for functional network imaging specifically at high spatial resolution. *NeuroImage*, 164, 214–229. <https://doi.org/10.1016/j.neuroimage.2017.03.002>

SUPPORTING INFORMATION

Additional supporting information may be found online in the Supporting Information section at the end of this article.

How to cite this article: Strik M, Shanahan CJ, van der Walt A, et al. Functional correlates of motor control impairments in multiple sclerosis: A 7 Tesla task functional MRI study. *Hum Brain Mapp*. 2021;42:2569–2582. <https://doi.org/10.1002/hbm.25389>